

Preparation of Samarium Oxide Nanoparticles Decorated Functionalized Multiwall Carbon Nanotubes Modified Electrode for the Electrochemical Determination of Catechol

Bhuvanenthiran Mutharani¹, Subramanian Sakthinathan², Shen-Ming Chen^{1,*}, Tse-Wei Chen^{1,*}, Te-Wei Chiu²

¹ Electroanalysis and Bioelectrochemistry Lab, Department of Chemical Engineering and Biotechnology, National Taipei University of Technology, No.1, Section 3, Chung-Hsiao East Road, Taipei 106, Taiwan (R.O.C).

² Department of Materials and Mineral Resources Engineering, National Taipei University of Technology, No.1, Section 3, Chung-Hsiao East Road, Taipei 106, Taiwan (R.O.C).

*E-mail: smchen78@ms15.hinet.net, tewei@ntut.edu.tw

Received: 23 February 2018 / Accepted: 18 April 2018 / Published: 5 June 2018

Herein, we describe the innovative and simple voltammetric method based on the samarium oxide (Sm_2O_3) decorated functionalized multiwall carbon nanotubes ($\text{Sm}_2\text{O}_3/\text{f-MWCNTs}$) using as an electrode material for the detection of catechol (CC). The as-prepared $\text{Sm}_2\text{O}_3/\text{f-MWCNTs}$ composite was confirmed by using scanning electron microscopy (SEM), energy dispersive X-ray spectroscopy (EDX) and fourier-transform infrared spectroscopy (FT-IR). The electrochemical properties of the $\text{Sm}_2\text{O}_3/\text{f-MWCNTs}$ were investigated by electrochemical impedance spectroscopy (EIS), cyclic voltammetry (CV) and differential pulse voltammetry (DPV). The as-proposed $\text{Sm}_2\text{O}_3/\text{f-MWCNTs}$ modified GCE exhibited an excellent electrocatalytic activity towards oxidation of CC. The electrochemical studies of DPV displays wide linear response range, lower detection limit and well sensitivity of 0.1-1249 μM , 0.03 μM and 0.213 $\mu\text{A}\mu\text{M}^{-1}\text{cm}^{-2}$, respectively. The as-prepared electrochemical sensor had good stability, repeatability and reproducibility for the determination of CC. Besides, the prepared electrode material modified GCE was successfully applied to the real sample analysis in various water samples and the obtained recovery from 94.5 to 99 % is confirm that the $\text{Sm}_2\text{O}_3/\text{f-MWCNTs}/\text{GCE}$ had better practical reliability to the determination of CC.

Keywords: Multiwall carbon nanotubes, Electrochemical sensor, Catechol, Differential pulse voltammetry, Low detection limit.

1. INTRODUCTION

Catechol (CC) is a class of benzene diols isomer and also used as main reagent for the organic synthesis [1]. Moreover, CC is used in different industrial applications including pesticides production,

perfumes manufacturing and pharmaceutical industries [2, 3]. In addition, the European Union (EU) and U.S Environmental Protection Agency (EPA), has classified (CC) as a human carcinogenic and environmental pollutant due to their low degradability and toxicity. Moreover, continues exposure of CC raises severe health problems to both human and animal such as affect the central nervous system and blood pressure [4-6]. Hence, the development of sensitive and selective methods for the low level detection of CC is more important. Currently, various analytical methods have been used for the determination of CC such as gas chromatography (GC), high performance liquid chromatography (HPLC), chemiluminescence, mass spectrometry, flow injection analysis and electrochemical methods. Among all, the electrochemical techniques offered many advantages including low cost, portability, and fast response technique than that of the other analytical methods [7-9]. However, the electrochemical determination of CC at bare glassy carbon electrode (GCE) has some problem due to the overlapping, low sensitivity and low charge transfer [10, 11]. To solve this problem, different materials have been used for the electrode modification such as graphene, carbon nanotubes, mesoporous carbon and carbon foams [12]. Especially, functionalized-multiwall carbon nanotubes (f-MWCNTs) used for the electrode materials due to their extraordinary physical and chemical properties such as a mechanical strength, large surface area, high chemical stability and excellent electrical conductivity [13-15]. Hence, they have applied to the various important applications, especially, sensors and energy storage devices. Furthermore, f-MWCNTs can be used as promising materials for catalyst with metal oxide and nanoparticles to form composites [16-18].

The oxides of rare earths elements (erbium, samarium, yttrium, europium, and cerium) have been widely applied to the variety of applications including sensor, electronic devices and catalysis. Moreover, the rare-earth oxide (REO) has some particular interest due to their small-size, quantum size, tunneling and interfacial effects. Especially, Sm_2O_3 nanoparticle (NPs) is one of the main rare earth oxide nanomaterials and used in high prominent applications in various fields such as nano-electronics, solar cells, semiconductor, sensors [19-21], gate dielectric in complementary metal–oxide–semiconductors (CMOS) and resistance random access memories (RRAMs) [31–35]. In this work, Sm_2O_3 NPs was incorporated on the f-MWCNTs surface and formation of composite. The conjugation between the Sm_2O_3 and f-MWCNTs was increased after formation of composite. The Sm_2O_3 /f-MWCNTs composite modified electrode displays enhanced electrocatalytic ability to the detection of CC.

2. EXPERIMENTAL SECTION

2.1. Materials and methods

Carboxylic acid functionalized multi-walled carbon nanotubes (f-MWCNTs; avg. diam. \times L 9.5 nm \times 1.5 μm), samarium (III) nitrate hexahydrate ($\text{Sm}(\text{NO}_3)_3 \cdot 6\text{H}_2\text{O}$), ammonium hydroxide (NH_4OH), potassium permanganate (KMnO_4), sulfuric acid (H_2SO_4) and hydrochloric acid (HCl) were purchased from Sigma-Aldrich Co Ltd. All other reagents were used without further purification. During the electrochemical experiment the electrolyte was purged with N_2 for 15 min to deoxygenation. All the reaction was used double distilled (DD) water and the electrochemical experiments were carried out at

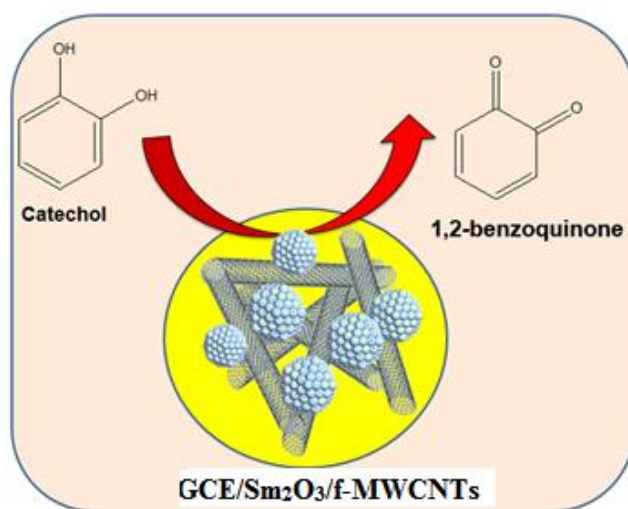
room temperature. The electrochemical studies were carried out by CHI 410 computerized electrochemical workstation. The electrochemical work station setup has platinum wire as an auxiliary electrode, GCE as a working electrode, and saturated Ag/AgCl as a reference electrode. The EIS studies were identified by ZAHNER (Kroanch, Germany) 0.1 Hz to 1 MHz frequency. The surface morphology of the sample was identified by Hitachi S-3000 FE-SEM measurements. FT-IR spectra were carried out by the JASCO FT/IR 6600 spectrometer.

2.2. Preparation of $\text{Sm}_2\text{O}_3/\text{f-MWCNTs}$ composite modified GCE

The two step manner was used to prepare the $\text{Sm}_2\text{O}_3/\text{f-MWCNTs}$ composites through the simple sonication method which was reported previously with slight modification [30]. The details about two step manners are given below. In the first step, to synthesize the $\text{Sm}_2\text{O}_3\text{NPs}$, 2g of Sm $(\text{NO}_3)_3 \cdot 6\text{H}_2\text{O}$ was added to 25 mL of DD and ultrasonication for 60 min, then, 30 % of NH_4OH liquid solution was added dropwise to the above solution during the reaction to form $\text{Sm}_2\text{O}_3\text{NPs}$. In the second step, 50 mL of f-MWCNTs (1g) was added to the Sm_2O_3 NPs under constant stirring for 30 min. Then, the above mixture was sonicated for 20 min. Finally, the obtained $\text{Sm}_2\text{O}_3/\text{f-MWCNTs}$ composite was washed with ethanol and DD water in several times via the centrifugation process with 6000 rpm. The collected samples were dried at oven and used for further experiments.

2.3. Fabrication of $\text{Sm}_2\text{O}_3/\text{f-MWCNTs}$ modified electrode GCE

For the modification, the bare GCE was polished with 0.05 μm alumina slurry and washed with DD water to remove the impurities on the electrode surface. The $\text{Sm}_2\text{O}_3/\text{f-MWCNTs}$ (2:1 ratio) composite was re-dispersed in DD water and sonicated for 30 min to get well dispersed homogeneous suspension.



Scheme 1. Preparation of $\text{Sm}_2\text{O}_3/\text{f-MWCNTs}$ composite modified GCE electrode and used for the CC detection.

Then, the 8 μL of $\text{Sm}_2\text{O}_3/\text{f-MWCNTs}$ composite suspension was coated on the mirror polished bare GCE surface and allowed to dry at room temperature. Moreover, the dried GCE was washed with DD water to remove loosely bounded $\text{Sm}_2\text{O}_3/\text{f-MWCNTs}$ particles on the GCE surface. Further, it can be used for all the electrochemical experiments (scheme 1).

3. RESULTS AND DISCUSSION

3.1. Characterization

Fig. 1 shows the FE-SEM images of (A) $\text{Sm}_2\text{O}_3\text{NPs}$, (B) $\text{Sm}_2\text{O}_3/\text{f-MWCNTs}$ composite and (C) f-MWCNTs. The SEM image of $\text{Sm}_2\text{O}_3\text{NPs}$ shows grains in the range of 15–20 nm.

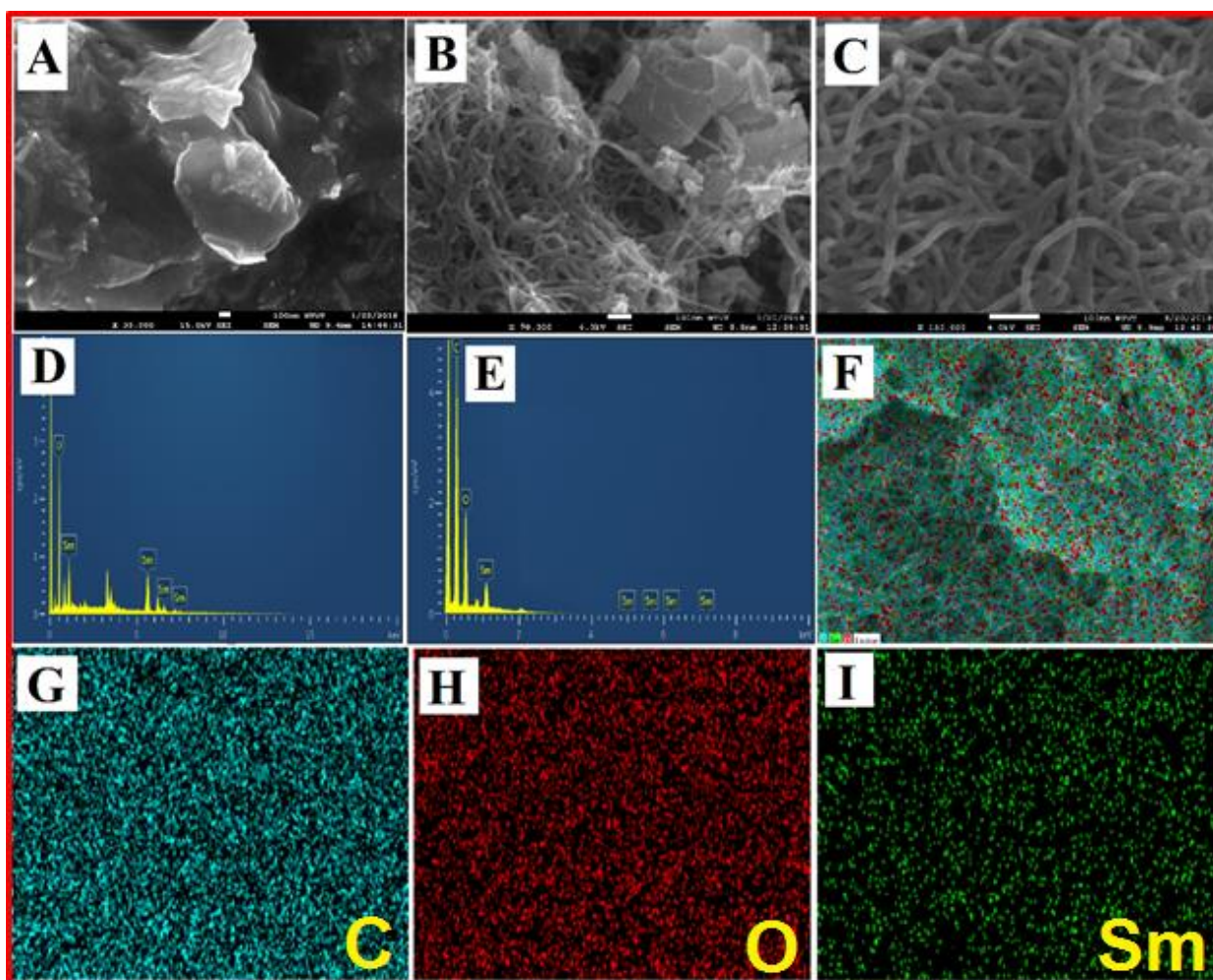


Figure 1. FE-SEM images of (A) Sm_2O_3 , (B) $\text{Sm}_2\text{O}_3/\text{f-MWCNTs}$ composite, (C) f-MWCNTs, (D) EDX spectra of Sm_2O_3 , (E) EDX spectra of $\text{Sm}_2\text{O}_3/\text{f-MWCNTs}$ composite, (F) EDX elemental mapping image of $\text{Sm}_2\text{O}_3/\text{f-MWCNTs}$ composite, (G), (H) and (I) elemental mapping images for C, O and Sm, respectively.

Fig. 1A shows the SEM image of Sm_2O_3 exhibit crumpled sheet structure and Fig. 1C shows the tube-like structure of f-MWCNTs. Moreover, Fig. 1B shows the SEM image of $\text{Sm}_2\text{O}_3/\text{f-MWCNTs}$ exhibits Sm_2O_3 anchored on the f-MWCNTs surfaces, which confirms the well interaction between the f-MWCNTs and Sm_2O_3 NPs. Fig. 1D and E indicates the EDX spectra of Sm_2O_3 and $\text{Sm}_2\text{O}_3/\text{f-MWCNTs}$, which confirms that the elements are present in the composite material. From the elemental mapping, Fig. 1F-I shows that the $\text{Sm}_2\text{O}_3/\text{f-MWCNTs}$ composite containing all elements such as carbon (C), oxygen (O) and samarium (Sm) in the composite materials.

FT-IR spectroscopy is an important technique to characterize the as-prepared composite. Fig. 2A exhibits the FT-IR spectra of (a) Sm_2O_3 , (b) $\text{Sm}_2\text{O}_3/\text{f-MWCNTs}$ composite. The FT-IR spectrum of Sm_2O_3 exhibits an O–H stretching vibration at 3500 cm^{-1} and stretching vibrations of C=O and C–O at 1730 cm^{-1} and 1050 cm^{-1} , respectively. The broad absorption band was observed in the region at 680 cm^{-1} which corresponds to the deformation mode of the Sm-O-H bonds in $\text{Sm}_2\text{O}_3 \cdot x\text{H}_2\text{O}$. The FT-IR spectrum of $\text{Sm}_2\text{O}_3/\text{f-MWCNTs}$ composite shows N–H vibrations at 3400 cm^{-1} and C–H stretching at 2925 cm^{-1} . Moreover, the bands at 1496 cm^{-1} and 1334 cm^{-1} were assigned to C=C and C–N stretching vibrations. This can be attributed to the strong interaction between the $\text{Sm}_2\text{O}_3/\text{f-MWCNTs}$ composite. In the FT-IR spectra of Sm_2O_3 band is observed at 680 cm^{-1} for the deformation mode of Sm-O-H band and 1625 cm^{-1} show for the bending mode of H_2O . The FT-IR spectrum of the f-MWCNTs shows the characteristic peak at 1705 cm^{-1} and a weaker band is observed at 1220 cm^{-1} due to the C=O and C–OH vibrations of the f-MWCNTs. In addition, the broad peak appeared at 3450 cm^{-1} for the O–H stretching vibrations. When the Sm_2O_3 was incorporated on the f-MWCNTs, the vibration bands of $\text{Sm}_2\text{O}_3/\text{f-MWCNTs}$ composite were shifted. Therefore, the changes of the vibration band confirmed the interaction between the f-MWCNTs and Sm_2O_3 NPs.

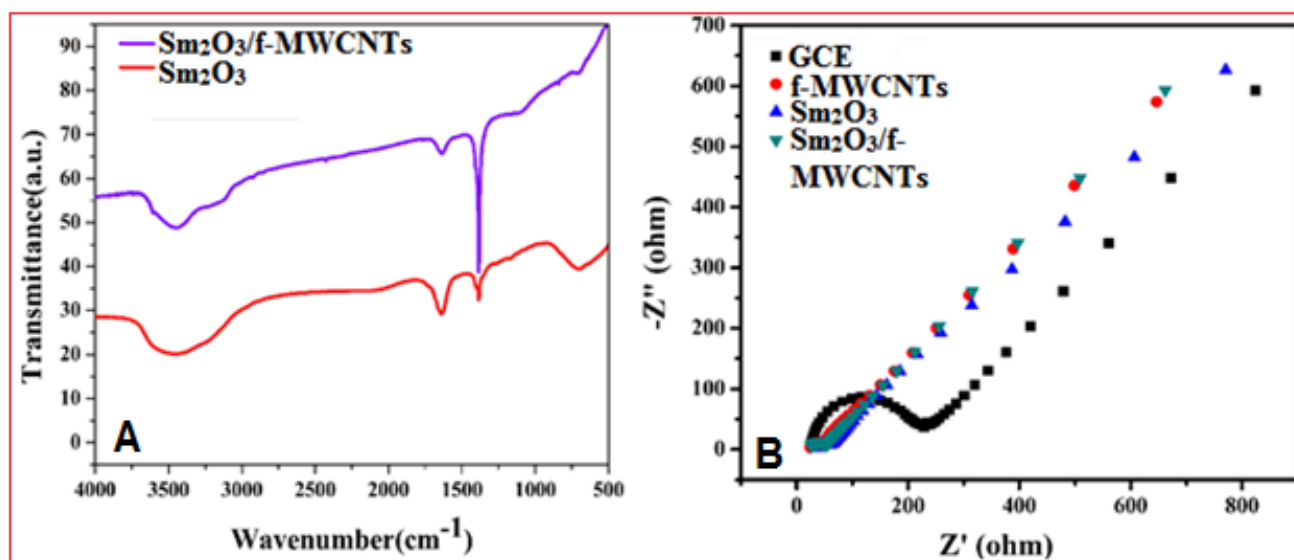


Figure 2. (A) IR spectra of (a) Sm_2O_3 , (b) $\text{Sm}_2\text{O}_3/\text{f-MWCNTs}$ composite. (B) EIS spectra of bare GCE, GCE/f-MWCNTs, GCE/ Sm_2O_3 , GCE/ $\text{Sm}_2\text{O}_3/\text{f-MWCNTs}$ composite modified electrodes in 0.1 M KCl containing 5 mM $[\text{Fe}(\text{CN})_6]^{3-/4-}$.

3.2. Electrochemical impedance spectroscopy (EIS)

EIS Nyquist plot (Fig.2B) of (a) bare GCE, (b) GCE/Sm₂O₃, (c) GCE/f-MWCNTs, (d) GCE/Sm₂O₃/f-MWCNTs composite modified electrodes in a 5mM [Fe(CN)₆]^{-3/-4} solution containing 0.1 M KCl as a supporting electrolyte and the frequency range between 100 MHz-100 KHz. The charge transfers resistance (R_{ct}) of modified electrode can be calculated by Nyquist plot fitting with the Randles equivalent circuit model. The bare GCE displayed a large semicircle with R_{ct} of 199.8 Ω , and this is attributed to poor conductivity. The GCE/Sm₂O₃ and GCE/f-MWCNTs modified electrodes shows R_{ct} values of 14.6 Ω and 20.2 Ω , respectively. The GCE/Sm₂O₃/f-MWCNTs composite modified electrode shows a small semicircle with low R_{ct} of 24.9 Ω due to the lower electrode resistance. Therefore, the low resistance of the modified electrode should be ascribed to the high electronic conductivity.

3.3. Electrocatalytic behavior of CC at different modified electrodes

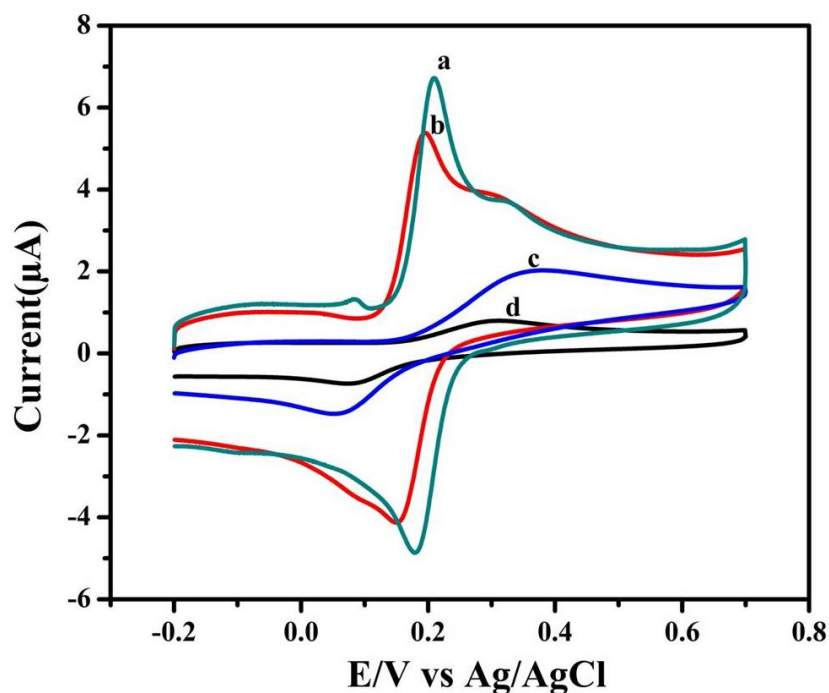


Figure 3. CV curve of (a) GCE/Sm₂O₃/f-MWCNTs modified, (b) GCE/f-MWCNTs, (c) GCE/Sm₂O₃, (d) bare GCE in 0.05 M PB solution (pH-7) containing 200 μ M CC at a scan rate 50 mV/s.

The electrochemical sensor performance of the different modified electrode towards the detection CC was identified by the CV in pH-7 in 0.05 M PBS, at a scan rate of 50 mV/s. Fig. 3 exhibit the electrocatalytic behavior of CC at (a) GCE/Sm₂O₃/f-MWCNTs modified, (b) GCE/f-MWCNTs, (c) GCE/Sm₂O₃, (d) bare GCE in the presence of 200 μ M CC. It was found that the bare GCE shows the lower peak current was observed for the oxidation of CC. Moreover, the GCE/f-MWCNTs electrode an exhibited the well redox peaks at $E_{pa} = 0.19$ V for oxidation and $E_{pc} = 0.14$ V for reduction peak with the corresponding peak current was found to be $I_{pa} = 5.37$ μ A, $I_{pc} = -4.140$ μ A, respectively. On

the other hand, the GCE/Sm₂O₃, fabricated electrode shows the CC oxidation peak at $E_{pa} = 0.37$ V, reduction peak at $E_{pc} = 0.05$ V with the respective peak current values about $I_{pa} = 2.06$ μ A and $I_{pc} = -1.516$ μ A. Interestingly, the GCE/Sm₂O₃/f-MWCNTs shows the enhanced oxidized and reduced peak appeared at $E_{pa} = 0.21$ V, $E_{pc} = 0.17$ V and the peak current of $I_{pa} = 6.74$ μ A, $I_{pc} = -4.887$ μ A. The obtained result shows that the GCE/Sm₂O₃/f-MWCNTs modified electrode exhibited an enhanced electrocatalytic activity for CC. The Sm₂O₃ combined with f-MWCNTs which is an increasing the electrocatalytic activity due to the interaction between the f-MWCNTs and Sm₂O₃ NPs. The excellent electrocatalytic activity and electrical conductivity of GCE/Sm₂O₃/f-MWCNTs modified electrode can be used for the detection of CC.

3.4. Effect of different pH and scan rate

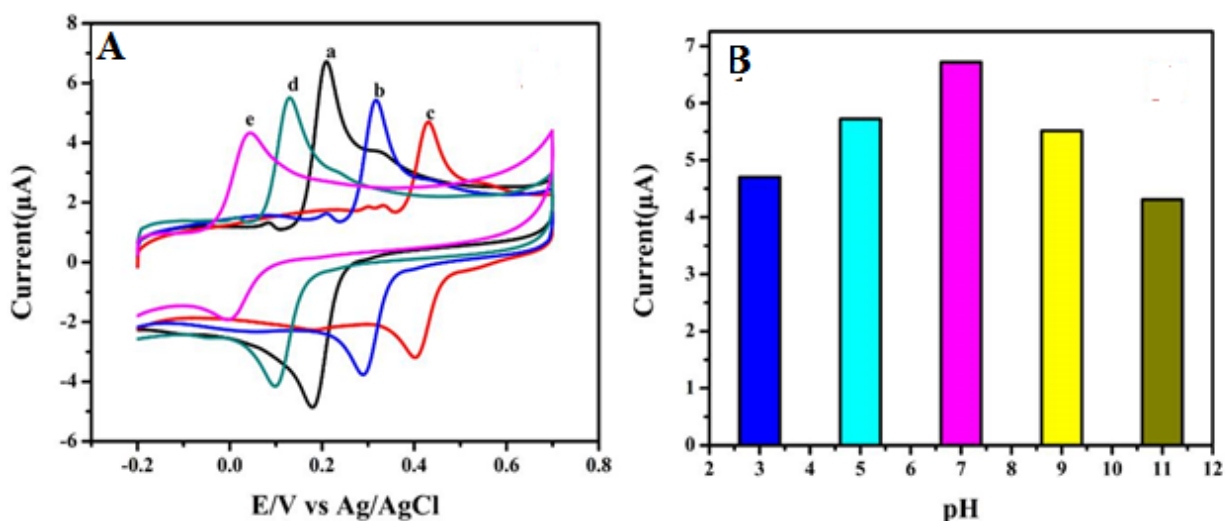


Figure 4. (A) CVs of the GCE/Sm₂O₃/f-MWCNTs modified in 200 μ M CC with different pH solutions (3, 5, 7, 9 & 11) at a scan rate of 50 mV/s, (B) the bar diagram of I_{pa} vs. pH.

In most of the case, the pH of the solution is significant influence factor to the electrochemical reactions. Fig. 4A exhibit the influence of pH on the electrochemical response of the GCE/Sm₂O₃/f-MWCNTs modified electrode was studied at different pHs (3 to 11) towards CC detection and the scan rate of 50 mV/s. It can be observed that the electrolyte pH influenced the peak current and peak potential of CC detection. In this studies, an increasing the pH value from 3 to 7, the peak current was increased, after certainly decreased at pH 9 - 11. Moreover, the peak potentials are moved negative to positive side with an increasing the pH value (3 to 11). Both the anodic peak potential (E_{pa}) and the cathodic peak (E_{pc}) of CC were proportional with the solution pH in the range of 3 to 11. These results suggest that the redox reaction of CC has the equal number of protons and electron transfer process at the GCE/Sm₂O₃/f-MWCNTs electrode. Moreover, the maximum peak current was obtained at pH-7 from the Fig.4B. Hence, the electrochemical performance of CC detection and other electrochemical studies were carried out at pH-7.

Fig. 5A shows the CV response of GCE/Sm₂O₃/f-MWCNTs modified electrode at different scan rate in the presence of 200 μ M CC in N₂ saturated pH-7 PB solution. The anodic and cathodic

peak current response was increased with increasing the scan rate between 10-300 mV/s. Moreover, an increasing the scan rates, the oxidation peaks current and the reduction peak current shifted to positive and negative potentials, respectively.

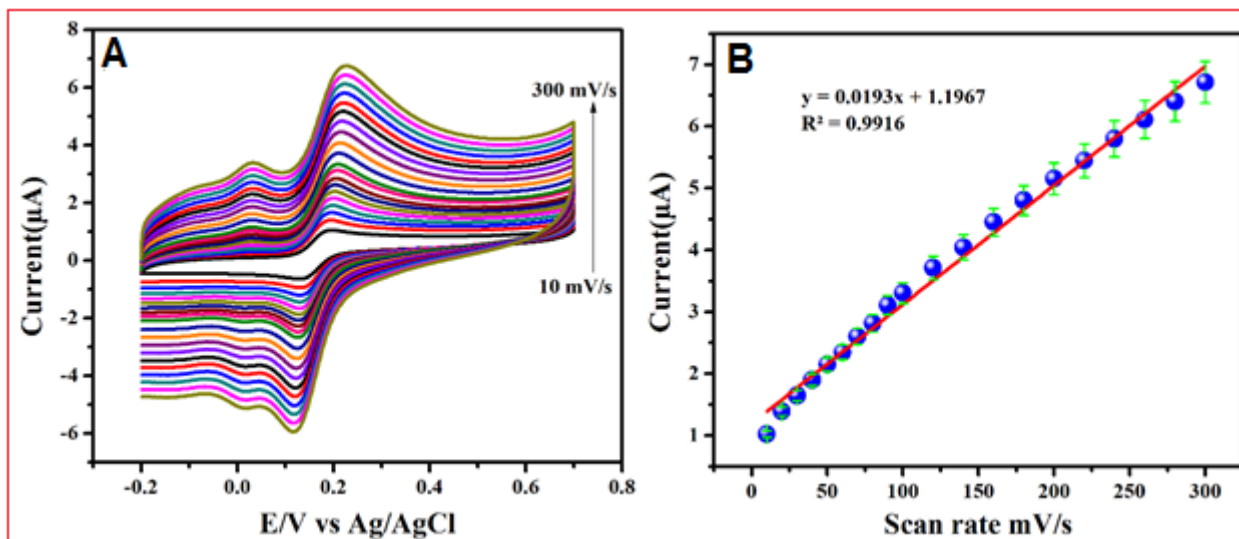


Figure 5. (A) Effect of scan rate at GCE/Sm₂O₃/f-MWCNTs modified electrode towards the detection of 200 µM CC in PBS (pH-7), (B) Linear plot of scan rate vs. anodic peak current.

3.5. Determination of CC

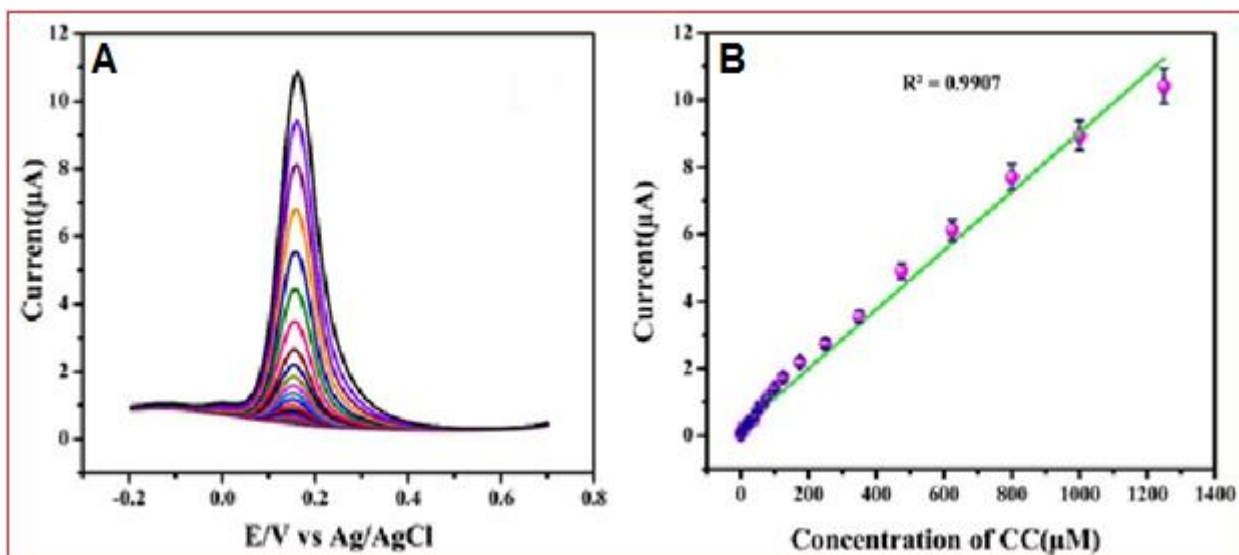


Figure 6. (A) DPV response for the different concentrations of CC at GCE/Sm₂O₃/f-MWCNTs modified electrode in PBS (pH-7). (B) Calibration plot between the different concentrations of CC vs. oxidation peak current.

Fig. 5B exhibited the linear regression equation for the anodic peak current was $I_{pa} = 0.019 + 1.196$ (mV/s) with a correlation coefficient of $R^2 = 0.991$. This indicates that the electrocatalytic reaction at the GCE/Sm₂O₃/f-MWCNTs modified electrode is an adsorption controlled and quasi reversible reaction.

DPV technique is more sensitive and suitable method than that of CV. Fig.6A shows DPV responses of CC oxidation on GCE/Sm₂O₃/f-MWCNTs modified electrode in 0.05 M PBS containing different addition of CC. The CC oxidation peak current was increased with increasing the different concentration of CC. Fig. 6B exhibit the linear calibration plot between the CC concentration and the peak current. Moreover, the linear concentration range of fabricated electrode is 0.1-1249 μM and the limit of detection (LOD) is 0.03 μM . In addition, the sensitivity of the GCE/Sm₂O₃/f-MWCNTs is calculated to be $0.213\mu\text{A}\mu\text{M}^{-1}\text{cm}^{-2}$, which is higher than that of the other previously reported modified electrodes as mentioned in the Table 1 such as, AuNP/CNF-GCE modified electrode (LOD = 0.36 μM) [22], MWNT/GCE fabricated electrode (LOD=0.6 μM) [23], PASA/MWNT/GCE electrode (LOD= 1 μM) [24], Integrated MWCNT electrode sensor (LOD 0.6 μM) [10], MWCNT-PMG/GCE modified electrode (LOD= 5.8 μM) [25], SWNT/GCE decorated modified electrode (LOD=0.26 μM) [26], CMK-3/GCE sensor electrode (LOD=0.1 μM) [27], Nano grass array BDD electrode (LOD= 1.3 μM) [28] and Graphene–chitosan/GCE (LOD= 0.75 μM). Hence, the obtained result shows that the prepared electrode had better performance for the electrochemical determination of CC due to the electron transfer and well electro catalytic properties of the GCE/Sm₂O₃/f-MWCNTs. Moreover, the GCE/Sm₂O₃/f-MWCNTs modified electrode has the large surface area and also well adsorption of CC. Therefore, the GCE/Sm₂O₃/f-MWCNTs composite modified electrode as an excellent electrocatalytic activity for the electrochemical detection of CC.

3.6. Reproducibility, repeatability and stability

Reproducibility and repeatability of the GCE/Sm₂O₃/f-MWCNTs modified electrode was identified by CV in 0.05 M PBS containing 0.1 μM CC. The as-prepared sensor shows an acceptable repeatability with relative standard deviation (RSD) of 2.23 % for repetitive measurements carried out using a single modified electrode. On the other hand, the GCE/Sm₂O₃/f-MWCNTs modified electrode exhibited satisfactory reproducibility of 2.98 % for five independent measurements carried out by five individual modified electrodes. After that, the storage stability of the sensor was monitored one-month storage period, the modified electrode shows a stable response towards the determination of CC with 76.12% of the initial CC response peak current was obtained after one month of its use which proof that the excellent storage stability of the prepared electrode.

3.7. Real sample analysis

In order to assess the practical utility of the sensor, we have measured the CC in real water samples like tap water and sea water by GCE/Sm₂O₃/f-MWCNTs modified electrode. Then the stock solution of CC was prepared by 0.05 M PBS (pH-7) and the known concentration of CC were spiked into real samples such as tap water and sea water. Moreover, the aforementioned samples were utilized to detect real samples. Furthermore, adding values and the recovery results were measured through a

standard addition method and it was displays in Table 2. From the recovery results, the GCE/Sm₂O₃/f-MWCNTs modified electrode has been applied to real sample analysis for the detection of CC.

Table 1. Comparison of analytical parameters of GCE/Sm₂O₃/f-MWCNTs modified for the detection of CC with previously reported electrodes

Electrodes	LOD (μM)	Linear range (μM)	Ref.
AuNP/CNF-GCE	0.36	5–350	[22]
MWNT/GCE	0.6	2–100	[23]
PASA/MWNT/GCE	1	6–700	[24]
Integrated MWCNT electrode	0.6	1–1000	[10]
MWCNT-PMG/GCE	5.8	30–1190	[25]
SWNT/GCE	0.26	0.4–10	[26]
CMK-3/GCE	0.1	0.5–35	[27]
Nano grass array BDD electrode	1.3	5–100	[28]
Graphene–chitosan/GCE	0.75	1–400	[29]
GCE/Sm ₂ O ₃ /f-MWCNTs	0.03	0.1-1249	This work

Table 2. Determination of CC in water sample by GCE/Sm₂O₃/f-MWCNTs modified electrode.

Sample	Added (μM)	Found (μM)	Recovery (%)
Tap water	0	-	-
	10	9.45	94.5
	20	19.5	97.5
Sea water	0	-	-
	10	9.81	98.1
	20	19.8	99

4. CONCLUSIONS

In summary, we have developed the GCE/Sm₂O₃/f-MWCNTs modified electrode was used for the selective and sensitive detection of CC. The as-prepared GCE/Sm₂O₃/f-MWCNTs electrode exhibit an enhanced peak current of CC than that of the other modified electrode. The GCE/Sm₂O₃/f-MWCNTs modified electrode shows the low LOD and high sensitivity. The obtained LOD and sensitivity are the best than the previously reported CC sensors. In addition, a good recovery of CC at GCE/Sm₂O₃/f-MWCNTs modified electrode authenticates that the developed sensor can be used as a

potential electrode material for the detection of CC. Moreover, the prepared sensor has been used for the determination CC in real sample analysis.

References

1. H. Rao, Y. Liu, J. Zhong, Z. Zhang, X. Zhao, X. Liu, Y. Jiang, P. Zou, X. Wang and Y. Wang, *ACS Sustain. Chem., Eng.*, 5 (2017) 10926.
2. L. A. Alshahrani, X. Li, H. Luo, L. Yang, M. Wang, S. Yan, P. Liu, Y. Yang and Q. Li, *Sensors.*, 14 (2014) 22274.
3. H. Zhang, S. Li, F. Zhang, M. Wang, X. Lin and H. Li, *J Solid State Electrochem.*, 21(2017) 735.
4. B. P. Lopezab and A. Merkoci, *Analyst.*, 134 (2009) 60.
5. Y. H. Huang, J. H. Chen, L. J. Ling, Z. B. Su, X. Sun, S. R. Hu, W. Weng, Y. Huang, W. B. Wu and Y. S. He, *Analyst.*, 140 (2015) 7939.
6. Y. Liang and J. Li, Y. Zhao, *Int. J. Electrochem. Sci.*, 12 (2017) 9512.
7. X. Li, G. Xu, X. Jiang and J. Tao, *J. Electrochem. Soc.*, 161 (2014) 464.
8. A. S. Kumar and P. Swetha, *Langmuir.*, 26 (2010) 6874.
9. M. Wei, Y. Liu, Z. Z. Gu and Z. D. Liu, *J. Chin. Chem. Soc.*, 58 (2011) 516.
10. S.G. Wang, Y.Q. Li, X.J. Zhao, J.H. Wang, J.J. Han and T. Wang, *Diam. Relat. Mater.*, 16 (2007) 248.
11. Y. Umasankar, A. P. Periasamy and S. M. Chen, *Anal. Biochem.*, 411 (2011) 71–79.
12. S. Sakthinathan, S. M. Chen and W. C. Liao, *Inorg. Chem. Front.*, 4 (2017) 809–819.
13. R. Karthik, R. Sasikumar, S.M. Chen, J. Vinoth Kumar, A. Elangovan, V. Muthuraj, P. Muthukrishnan, Fahad M.A. Al-Hemaid, M. A. Ali and M. S. Elshikh, *J. Colloid Interface Sci.* 487 (2017) 289.
14. A. Saha, A. Moya, A. Kahnt, D. Iglesias, S. Marchesan, R. Wannemacher, M. Prato, Juan J. Vilatela and D. M. Guldi, *Nanoscale.*, 9 (2017) 7911.
15. G. Tuci, L. Luconi, A. Rossin, E. Berretti, H. Ba, M. Innocenti, D. Yakhvarov, S. Caporali, C. P. Huu and G. Giambastiani, *ACS Appl. Mater. Interfaces.*, 8 (2016) 30099.
16. M. Amirian, A. N. Chakoli, W. Cai and J. Sui, *Sci. Iran.*, 20 (2013) 1023.
17. N. Wang, Y. Feng, L. Zeng, Z. Zhao and T. Chen, *ACS Appl. Mater. Interfaces.*, 7 (2015) 14933.
18. A. S. Dezfali, M. R. Ganjali and H. R. Naderi, *Appl. Surf. Sc.i.*, 402 (2017) 245.
19. W. Zhu, L. Xu, J. Ma, R. Yang and Y. Chen, *J. Colloid Interface Sci.*, 340 (2009) 119.
20. J. D. Qiu, W. M. Zhou, J. Guo, R. Wang and R. P. Liang, *Anal. Biochem.*, 385 (2009) 264.
21. Z. Xu, X. Chen, X. Qu and S. Dong, *Electroanalysis.*, 16 (2004) 684.
22. Z.H. Huo, Y.L. Zhou, Q. Liu, X.L. He, Y. Liang and M.T. Xu, *Microchim. Acta.*, 173 (2011) 119.
23. Y.P. Ding, W.L. Liu, Q.S. Wu and X.G. Wang, *J. Electroanal. Chem.*, 575 (2005) 275.
24. D.M. Zhao, X.H. Zhang, L.J. Feng and S.F. Wang, *Colloid Surf. B.*, 74 (2009) 317.
25. Y. Umasankar, A.P. Periasamy and S.M. Chen, *Anal. Biochem.*, 411 (2011) 71.
26. Z.H. Wang, S.J. Li and Q.Z. Lv, *Sens. Actuators B: Chem.*, 127 (2007) 420.
27. J.J. Yu, W. Du, F.Q. Zhao and B.Z. Zeng, *Electrochim. Acta.*, 54 (2009) 984.
28. M. Lv, M. Wei, F. Rong, C. Terashima, A. Fujishima and Z.Z. Gu, *Electroanalysis.*, 22 (2010) 199.
29. H.S. Yin, Q.M. Zhang, Y.L. Zhou, Q. Ma, T. Liu, L.S. Zhou and S.Y. Ai, *Electrochim. Acta.*, 56 (2011) 2748.
30. A. S. Dezfali, M. R. Ganjali, H. Jafari and F. Faridbod, *J Mater Sci: Mater Electron.*, 28 (2017) 6176.
31. W.C. Chin, K.Y. Cheong and Z. Hassan, *Materials Sci. Semicond. Process.*, 13 (2010) 303.
32. S.-Y. Huang, T.-C. Chang and M.-C. Chen et al., *Solid State Electron.*, 189 (2011) 63.
33. M.-H. Wu, C.-H. Cheng, C.-S. Lai and T.-M. Pan, *Sens. Actuators, B.*, 221 (2009) 138.
34. C.R. Michel, A.H. Martínez-Preciado, R. Parra, C.M. Aldao and M.A. Ponce, *Sens. Actuators, B.*,

1220 (2014) 202.

35. J.-G Kang, B.-K Min and Y. Sohn, *J Mater Sci.*, 1958 (2015) 50.

© 2018 The Authors. Published by ESG (www.electrochemsci.org). This article is an open access article distributed under the terms and conditions of the Creative Commons Attribution license (<http://creativecommons.org/licenses/by/4.0/>).